Simulation of adaptive feedforward control for magnetic alloy cavity

Xiang Li , Yang Liu

Institute of High Energy Physics, Beijing, China

Spallation Neutron Source Science Center, Dongguan, Guangdong, China

1.Introduction

The China Spallation Neutron Source (CSNS) comprises an 80 MeV low-energy H- linac, a 1.6 GeV rapid cycling synchrotron, and a target station. In subsequent upgrade plans, the second phase of the CSNS will elevate the beam power from 100 kW to 500 kW. The rapid cycling synchrotron RF system will incorporate three magnetic alloy cavities to supply fundamental and second harmonics to mitigate the space charge effects during injection and the early stages. The relevant RF parameters are shown in Table 1.

Table 1. RF parameters comparison between CSNS and CSNS-II.

	CSNS	CSNS-II
repetition rate / Hz	25	
beam power / kW	100	500
injection energy / MeV	80	300
extraction energy /GeV	1.6	
protons per pulse / 10^{13}	1.56	6.24
RF frequency / MHz	1.02-2.44	1.71-2.44
circulating current /A	1.5-3.6	12.6-18
number of RF cavities	8 (fundamental harmonic)	8(fundamental harmonic) 3(2^{nd} harmonic)

With the enhancement of beam power, the beam loading effects in the RCS will be notably intensified. This poses significant challenges for the control system. Since the broadband magnetic alloy cavity do not require tuning, direct feedback becomes challenging to implement. The power source system's nonlinearity at high power levels also constrains the utilization of beam feed-forward. To address these challenges, we have developed an adaptive feedforward with the aim of improving system control precision under the conditions of strong beam loading effects and high power system nonlinearity.

2. Algorithm studied by Simulink

System Modeling

Given that the magnetic alloy cavity is a broadband system, modeling the system using transfer functions is quite challenging. Therefore, based on the measured impedance data, we modeled the magnetic alloy cavity using Simulink shown in Fig.2. And an adaptive feedforward algorithm based on Simulink was established according to Fig.3.

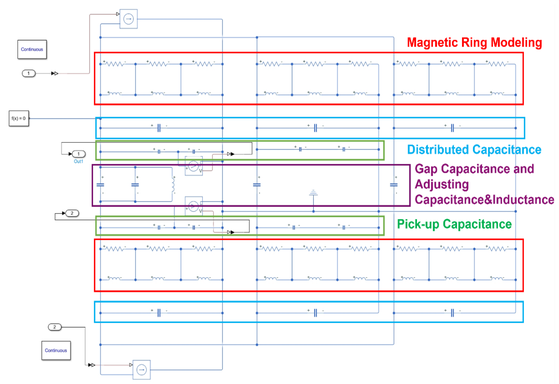

Figure 2. The magnetic alloy cavity modeling

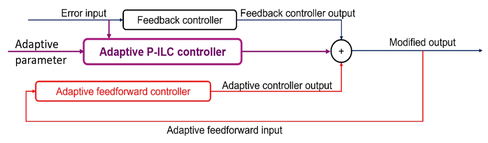

Figure 3. The flow and operation of the adaptive feedforward module.

Feedforward Signal Processing

Based on the ILC convergence conditions, the H-infinity (H∞) can be calculated for the system, which indicates that the filter bandwidth needs to be below 5kHz. The Fig.4 shows H∞ for various filters.

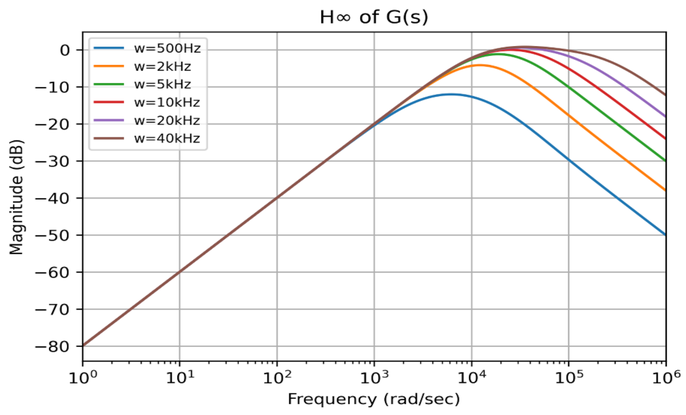

Figure 4. H∞ for various filters.

Using a conventional IIR filter introduces phase-lag, but using a zero-phase filter avoids this issue. We used a low-pass zero-phase filter with an 5kHz cutoff for the feedback signals.

Simulation Results

When the filter bandwidth exceeded 5kHz, oscillations occurred during the iterations. However, when the bandwidth was set to 5kHz, the system remained stable, this is consistent with the theoretical results. Based on theoretical analysis and practical simulations, setting the filter bandwidth to 5kHz proved to be feasible. The control error after taking adaptive feedforward for five iterations is shown Fig.5.

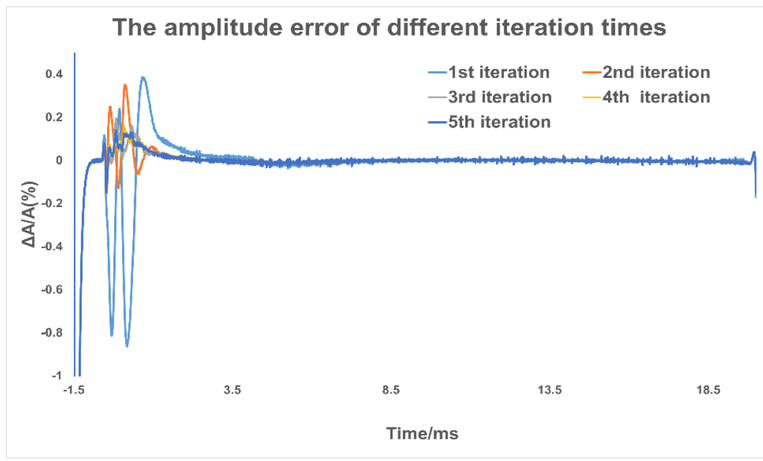

Figure 5. The control error in 5 times iteration.

Comparative graphs depicting the control accuracy between the combined approach of adaptive feed-forward and adaptive P-ILC, versus using just the adaptive feed-forward or adaptive P-ILC are presented in Fig.6.

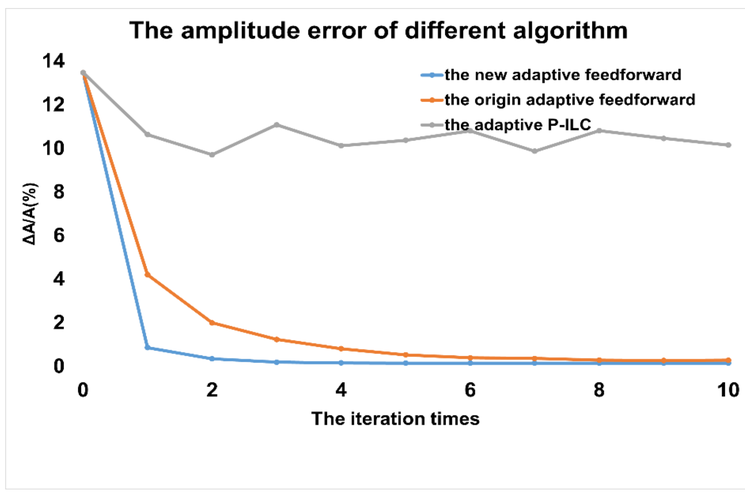

Figure 6. The control accuracy of different algorithms.

Upon employing the new adaptive feed-forward, the system's convergence speed significantly increased, and the control accuracy was also enhanced.

3. Summary and future work

The simulation results indicate that the use of the new adaptive feedforward has effectively improved the system's convergence speed and control accuracy. However, the simulation process cannot simulate the saturation distortion of the power source at high power and the beam loading effect. This optimization scheme still needs to be validated in the future and will be evaluated for the long-term performance of the improved feedforward control in the actual LLRF system. In addition, theoretical analysis will be conducted to study the impact of the new adaptive feedforward on control stability, convergence, and accuracy.

References

Liu H, Wang S. Longitudinal beam dynamic design of 500 kW beam power upgrade for CSNS-II RCS[J]. Radiation Detection Technology and Methods, 2022, 6(3): 339-348.

Li, X., Sun, H., Zhang, CL. et al. Design of rapid tuning system for a ferrite-loaded cavity. Radiat Detect Technol Methods 5, 324–331 (2021).

Tamura F, Sugiyama Y, Yoshii M, et al. Multiharmonic vector rf voltage control for wideband cavities driven by vacuum tube amplifiers in a rapid cycling synchrotron[J]. Physical Review Accelerators and Beams, 2019, 22(9): 092001.

Li S, Fang Z, Futatsukawa K, et al. Iterative learning control-based adaptive beam loading compensation im-plementations in the J-PARC LINAC[J]. Nuclear Instru-ments and Methods in Physics Research Section A: Ac-celerators, Spectrometers, Detectors and Associated Equipment, 2019, 945: 162612.

LI, SONG. "Development of Adaptive Compensation of Heavy Beam Loading for J-PARC LINAC." (2019).